

<https://doi.org/10.1038/s42003-025-07918-y>

IL-27 alleviates high-fat diet-induced obesity and metabolic disorders by inhibiting adipogenesis via activating HDAC6



Yinsheng Zhong^{1,2}, Shujun Yang^{1,2}, Shuangmei Li^{1,2}, Sijun Yuan¹, Xuxiang Chen¹, Huibao Long¹, Haidong Wu¹, Yajie Guo¹✉ & Tong Wang¹✉

Obesity arises from an imbalance between adipogenesis and adipocyte thermogenesis. Interleukin-27 (IL-27), a heterodimer cytokine, is known to promote thermogenesis in brown adipose tissue. However, its role in adipogenesis remains unclear. This study aims to investigate the effects of IL-27 on adipogenesis both in vitro and in vivo, and to elucidate the underlying mechanisms. In vitro, an adipogenic differentiation model of adipose-derived mesenchymal stem cells (ADSCs) demonstrate that IL-27 is non-cytotoxic to ADSCs and inhibits ADSCs adipogenic differentiation. In vivo, using a high-fat diet (HFD)-induced obese mouse model and a targeted adipose tissue-specific IL-27 overexpression adeno-associated viral (AAV) vector, we confirm that IL-27 suppresses adipogenesis, prevents weight gain, and improves glucose and lipid metabolic homeostasis in obese mice. Additionally, the inhibition of adipogenesis by IL-27 is mediated through HDAC6 activation of the TGF β /Smad3 signaling pathway. Our study suggests that IL-27 is a potential therapeutic target for obesity and metabolic disorders.

Obesity rates are escalating globally, with approximately 1.12 billion adults projected to be affected by 2030¹. Obesity is a multifaceted disease that leads to adipose tissue dysfunction and increases the risk of cardiovascular and metabolic disorders^{2,3}. Current therapeutic strategies for obesity focus on inhibiting adipogenesis, enhancing energy expenditure, and reducing adipose tissue inflammation⁴. Consequently, there is an urgent need to develop new therapeutic targets and widely accessible treatments for obesity and its related comorbidities.

Obesity is characterized by a significant enlargement in adipocyte volume (hypertrophy) and an increase in adipocyte number (hyperplasia)⁵. Adipose tissue-derived mesenchymal stem cells (ADSCs) are progenitors of adipocytes located in the stroma of adipose tissue⁶. The adipogenic differentiation of ADSCs is a complex process involving their transformation into mature adipocytes, which requires the coordinated activation of transcription factors such as CCAAT/enhancer-binding protein α (C/EBP α) and peroxisome proliferator-activated receptor γ (PPAR γ)⁷. The positive feedback regulation of C/EBP α and PPAR γ sustains their high expression levels during adipogenic differentiation⁸. Therefore, inhibiting the expression of C/EBP α and PPAR γ may present a potential therapeutic strategy for obesity.

Epstein-Barr virus-induced 3 (EBI3) and p28 form a heterodimer known as interleukin-27 (IL-27). It exerts dual roles in regulating inflammation in target cells by signaling through the IL-27 receptor, composed of IL-27R α (also known as WSX1) and gp130^{9,10}. Activated antigen-presenting cells, such as macrophages and dendritic cells, are the main producers of IL-27¹¹. IL-27R α is expressed in various cell types, including B cells, T cells, hematopoietic stem cells, and mesenchymal stem cells^{12,13}. According to recent research, IL-27 may be involved in metabolic diseases. Notably, there is a negative correlation between insulin resistance and obesity and human serum IL-27 levels^{14–16}. Further research indicates that systemic delivery of exogenous IL-27 plasmid can inhibit weight gain in high-fat diet-induced (HFD) obese mice¹⁷. This effect is likely due to IL-27's ability to directly promote thermogenesis in adipocytes¹⁸. Although some studies have confirmed the role of IL-27 in metabolic diseases, it remains unclear whether IL-27 can treat obesity by inhibiting the adipogenic differentiation of ADSCs.

In this work, we examined the role of IL-27 and its potential mechanisms in adipogenesis. By evaluating the expression levels of adipogenic markers, we determined that IL-27 could inhibit adipogenesis, suppress weight gain, and improve the balance of lipid and glucose homeostasis

¹Department of Emergency, The Eighth Affiliated Hospital of Sun Yat-sen University, Shenzhen, Guangdong, 518003, PR China. ²These authors contributed equally: Yinsheng Zhong, Shujun Yang, Shuangmei Li. ✉e-mail: guoyj36@mail.sysu.edu.cn; tongwang316@163.com

through HDAC6 in HFD obese mice. These findings suggest that IL-27 could be a promising therapeutic drug for obesity.

Results

IL-27 signaling is downregulated during adipogenic differentiation

To explore the differentially expressed genes during the process of adipogenic differentiation, we collected three datasets related to the process of adipogenic differentiation of human ADSCs from the GEO database (Supplementary Table 1)^{19–21}. Using R packages for data screening and

analysis, we identified 1837 differentially expressed genes in the GSE125331 dataset (Fig. 1A), 1522 differentially expressed genes in the GSE198481 dataset (Fig. 1B), and 2664 differentially expressed genes in the GSE249195 dataset (Fig. 1C). It is believed that chronic inflammation contributes to the regulation of obesity²². To investigate the expression patterns of interleukin cytokines during adipogenic differentiation, we found no common interleukin genes among the upregulated genes (Fig. 1D). However, there were two commonly downregulated interleukin genes, namely IL-6 and IL-27Rα (Fig. 1E). The role of IL-6 in adipogenic differentiation of ADSCs has been previously reported²³, while the effect of IL-27 signaling in regulating

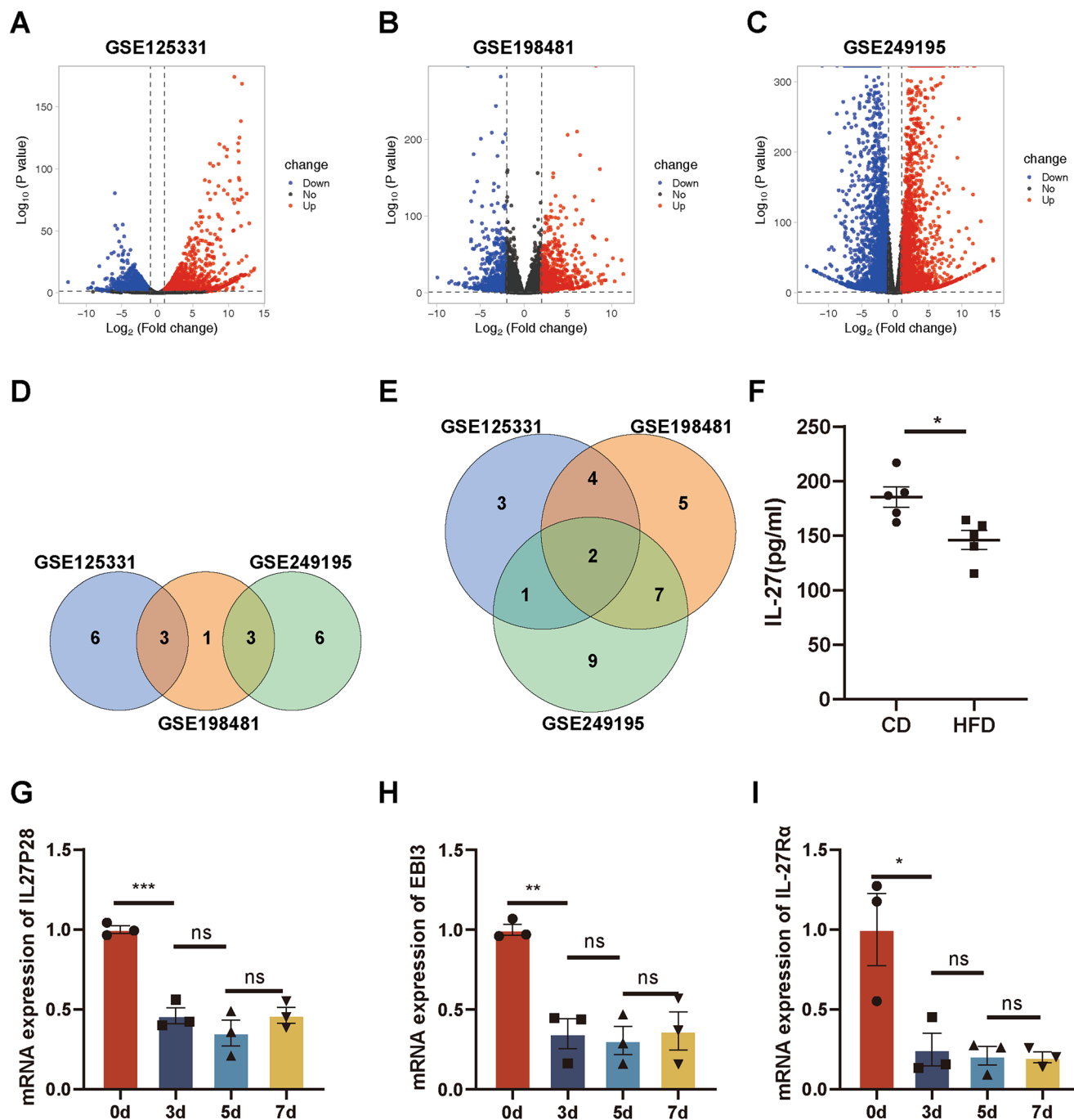


Fig. 1 | IL-27 signaling is downregulated during ADSC adipogenic differentiation. A–C Volcano plots of differentially expressed genes in three human ADSC adipogenic differentiation datasets. D Commonly upregulated genes in the adipogenic differentiation process among the three datasets. E Commonly downregulated genes in the adipogenic differentiation process among the three datasets. F Serum

IL-27 expression levels in high-fat diet-induced obese mice and normal diet-fed mice (n = 5). G–I Relative mRNA levels of IL27p28, EBI3, and IL-27Rα (n = 3). (Data are presented as the mean ± SEM, t-test between two groups, one-way ANOVA with Tukey's test between three or more groups. *p < 0.05, **p < 0.01, ***p < 0.001, ****p < 0.0001, ns no significance).

adipogenic differentiation remains unknown. We further detected the expression level of circulating IL-27 in HFD-induced obese mice and found that it was decreased in the serum of HFD mice (Fig. 1F). Additionally, we isolated and identified primary ADSCs from the adipose tissue of C57BL/6J mice (Supplementary Fig. S1). After successfully constructing an adipogenic differentiation model (Supplementary Fig. S2), we observed that the mRNA expression of IL27p28, EBI3, and IL-27Ra were downregulated on day 3 of differentiation and remained at low levels thereafter (Fig. 1G–I).

IL-27 exhibits no cytotoxic effects on ADSC proliferation

To investigate whether IL-27 affects ADSC proliferation and toxicity, we measured cell viability and cytotoxicity using EdU and CCK-8 assay after treatment with exogenous recombinant IL-27 protein. The EdU assay confirmed that different doses of IL-27 (25, 50, 100, and 200 ng/mL) did not affect DNA synthesis in ADSCs (Fig. 2A, B). Furthermore, in the CCK-8 assay, no significant differences in cell viability were observed at 24 h, 48 h, 72 h, or 96 h of treatment with varying IL-27 concentrations (Fig. 2C). These results indicated that IL-27 did not exhibit noticeable cytotoxicity on ADSC.

IL-27 inhibits ADSC adipogenic differentiation

We further evaluated the effect of IL-27 on ADSC adipogenic differentiation. ADSCs were treated with IL-27 (25, 50, 100, and 200 ng/mL) during adipogenic differentiation for 7 days. It was found that IL-27 (100 ng/mL) significantly inhibited lipid droplet formation (Fig. 2D, E), indicating an inhibitory effect on adipogenic differentiation. Additionally, the mRNA expression of adipogenic differentiation markers PPAR γ , C/EBP α , and FABP4 was downregulated (Fig. 2F–H). Protein levels of these adipogenic markers also decreased on days 3, 5, and 7 of differentiation induction with IL-27 (100 ng/mL) treatment (Fig. 2I–L). These results suggested that IL-27 could suppress adipogenic differentiation.

IL-27 reduces body weight and improves metabolic disorders in HFD-fed mice

To further evaluate the impact of IL-27 on metabolic homeostasis during obesity development in C57BL/6J mice, we first confirmed the successful construction of the HFD-induced obese mouse model. Subsequently, we constructed an adipose tissue-specific IL-27 overexpression vector (AAV2/9-FABP4-IL27). This vector-mediated IL-27 was successfully overexpressed in adipose tissue through tail vein injection (Supplementary Fig. S3). During the 12-week HFD feeding period, we observed that the weight gain of mice in the AAV-IL27 group was significantly inhibited from week 7 onwards (Fig. 3A). We recorded the food intake of both groups and found no differences (Fig. 3B). Body composition analysis using the QMR06-090H imaging system showed that the fat tissue content in the HFD + AAV-IL27 group was significantly lower than that of the control group (Fig. 3C–F), but there was little difference in lean mass between the two groups (Fig. 3G). This indicates that IL-27 can inhibit HFD-induced adipose tissue accumulation. Chronic inflammation in adipose tissue induced by HFD feeding impairs glucose homeostasis. To learn more about the effect of IL-27 on glucose metabolism in HFD-induced obese mice, we conducted GTT and ITT. IL-27 improved glucose metabolism, as evidenced by lower peak blood glucose and a 29.9% reduction in the mean area under the curve (AUC) in the HFD + AAV-IL27 group compared to the control group. (Fig. 3H, I). The insulin tolerance test also confirmed higher insulin sensitivity in the HFD + AAV-IL27 group, especially 15 minutes after insulin injection (Fig. 3J, K). Additionally, the total cholesterol levels in the HFD + AAV-IL27 group were significantly lower than those in the control group (Fig. 3L), although the total triglycerides showed no significant differences, only a potential downward trend (Fig. 3M).

IL-27 inhibits adipogenic differentiation of ADSC via HDAC6

Given the pivotal role of the HDAC family in adipogenesis^{24–26}, we investigated the changes in HDAC mRNA levels following IL-27 (100 ng/mL) treatment during ADSC adipogenic differentiation. We found that IL-27 significantly upregulated HDAC6 mRNA expression (Fig. 4A). Subsequent

protein analysis on days 3, 5, and 7 of adipogenic differentiation confirmed that IL-27 promoted HDAC6 protein levels (Fig. 4B, C). Since IL-27 works by attaching to its unique receptor IL-27R α , we hypothesized that HDAC6 might act as a regulatory hub in IL-27 signaling. Co-IP assay in C3H10T1/2 cell line revealed a direct interaction between IL-27R α and HDAC6, with IL-27 treatment enhancing this interaction (Fig. 4D, E and Supplementary Fig. S4). To clarify whether IL-27 inhibits adipogenic differentiation via HDAC6, we used Tubastatin A (TA), a specific inhibitor of HDAC6, at a concentration of 5 μ M²⁷. Inhibiting HDAC6 during adipogenic differentiation significantly increased the area stained with Oil Red O (Fig. 4F, G). Western blot examination showed elevated expression of adipogenic markers PPAR γ and C/EBP α upon HDAC6 inhibition by TA (Fig. 4H–K). These results indicated that IL-27's inhibition of adipogenic differentiation partially depends on HDAC6.

IL-27 inhibits adipogenic differentiation through HDAC6-mediated TGF β /Smad3 pathway activation in vitro

The Wnt/ β -catenin, PI3K/Akt, and TGF- β /Smad3 pathways are crucial in mesenchymal stem cell adipogenesis^{19,28,29}. Upon TA treatment, the expression level of HDAC6 was inhibited (Fig. 5A, B). IL-27 had no impact on the expression of β -catenin (Fig. 5A, C) but promoted the expression level of p-Akt. However, TA did not affect p-Akt. (Fig. 5A, D). Interestingly, IL-27 increased p-Smad3 expression, which was attenuated by TA (Fig. 5A, E, F). To verify the role of IL-27 via the TGF β /Smad3 signaling pathway in adipogenic differentiation, we used the TGF β receptor kinase inhibitor SB-431542 (SB) (10 μ M)³⁰, which significantly increased adipogenesis (Fig. 5G, H). SB reduced p-Smad3 expression without altering HDCA6 levels (Fig. 5I–L), accompanied by elevated adipogenic markers (Fig. 5I, M, N). This indicated that IL-27 promotes p-Smad3 expression through HDAC6. Collectively, our results demonstrate that IL-27 inhibits ADSC adipogenic differentiation by activating the TGF β /Smad3 signaling pathway via HDAC6.

IL-27 inhibits adipogenesis via HDAC6/TGF β /Smad3 pathway in vivo

To further elucidate the effects and mechanisms of IL-27 on adipogenesis in HFD mice, we performed anatomical and histopathological analyses of adipose and liver tissues. The overall white adipose tissue in different parts of the HFD + AAV-IL27 group was significantly smaller than that of the control group (Fig. 6A). Hematoxylin and eosin (HE) staining revealed that the fat content (triglycerides and other lipids) in the white adipose tissues of the inguinal, epididymal, and scapular regions were significantly reduced in the HFD + AAV-IL27 group (Fig. 6B–G). Adipocyte size and number were both lower than those in the control group (Fig. 6H, I).

Additionally, liver sections stained with Oil Red O and H&E revealed that hepatic fat deposition was significantly lower in the HFD + AAV-IL27 group than in the control group (Fig. 6J–M). The results indicate that IL-27 has the ability to suppress the formation of white adipose tissue in mice. To verify the changes in signaling pathways in adipose tissue, we extracted proteins from the inguinal white adipose tissue. In the HFD + AAV-IL27 group, the HDAC6 protein expression was elevated (Fig. 6N, O) as well as TGF β R1 and the phosphorylation of Smad3 (Fig. 6N, P, Q). The expression of PPAR γ and C/EBP α was decreased (Fig. 6N, R, S). Taken together, we found that IL-27 effectively inhibits adipogenesis through HDAC6-mediated activation of the TGF β /Smad3 pathway.

Discussion

IL-27, belonging to the IL-12 family, plays a significant role in innate immunity and inflammatory responses in autoimmune diseases^{31,32}. Sub-clinical chronic inflammation is believed to originate from adipose tissue³³. Our study highlights that IL-27 expression is downregulated during adipogenic differentiation of ADSCs. In vitro experiments revealed that exogenous IL-27 inhibits ADSCs adipogenesis by activating the TGF β /Smad3 signaling pathway via HDAC6 without affecting ADSCs proliferation. Additionally, targeted overexpression of IL-27 in adipose tissue inhibited

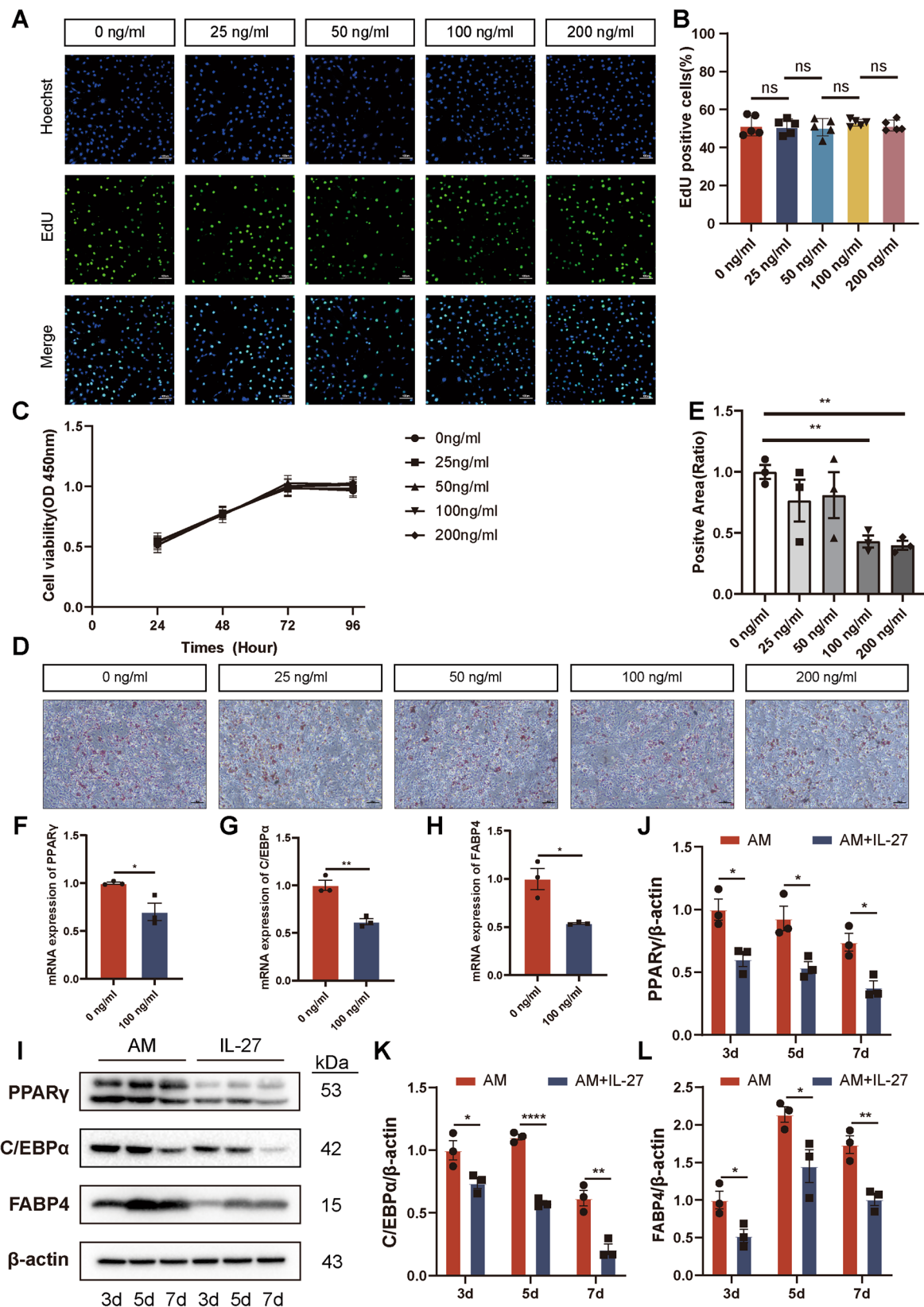


Fig. 2 | The inhibitory effect of IL-27 on ADSC adipogenic differentiation. **A, B** EdU assay to assess the effect of IL-27 on ADSC proliferation at 24 hours (n = 5, scale bar = 100 μm). **C** CCK-8 assay to determine the effect of IL-27 on ADSC proliferation at 24, 48, 72, and 96 hours. **D, E** Oil Red O staining results on day 7 of adipogenic differentiation (n = 3, scale bar = 100 μm). **F–H** Relative mRNA levels of

PPARγ, C/EBPα, and FABP4 (n = 3). **I–L** Western blot bands and integral optical density (IOD) analysis of PPARγ, C/EBPα, and FABP4 on days 3, 5, and 7 of adipogenic differentiation (n = 3). (Data are presented as the mean ± SEM, t-test between two groups, one-way ANOVA with Tukey's test between three or more groups. *p < 0.05, **p < 0.01, ***p < 0.001, ****p < 0.0001, ns no significance).

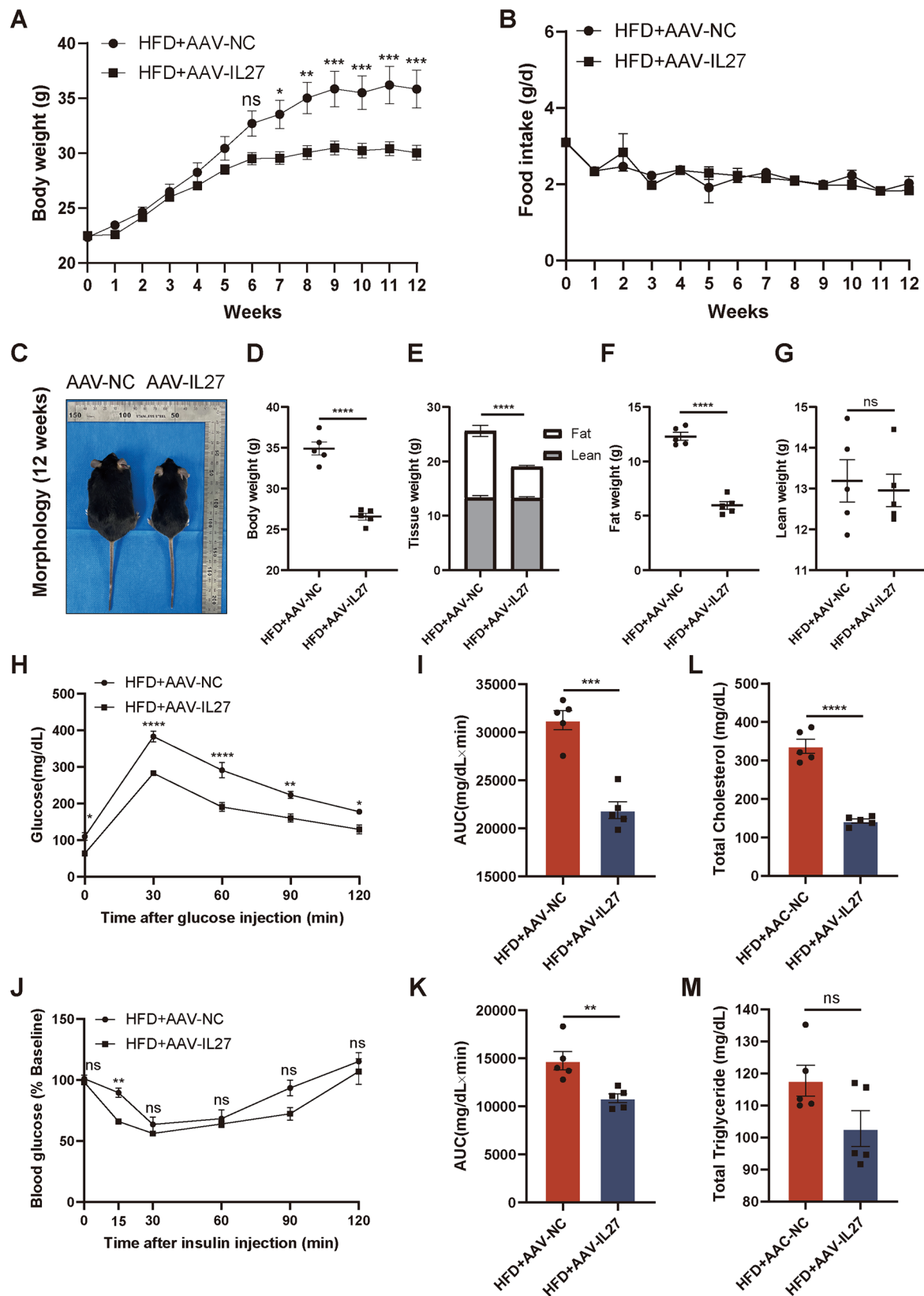


Fig. 3 | IL-27 reduces body weight in HFD-fed mice and improves glucose and lipid metabolism. Male C57BL/6J mice were randomly assigned to the HFD + AAV-NC or HFD + AAV-IL27 groups. At the start of the experiment, adeno-associated virus overexpression or control vectors were administered via tail vein injection. HFD feeding continued for 12 weeks. **A, B** Line charts of mouse body weight and food intake ($n = 5$). **C, D** Representative photographs of mice and body

weight analysis ($n = 5$). **E–G** Analysis of fat and lean mass in mice ($n = 5$). **H, I** GTT ($n = 5$). **J, K** ITT ($n = 5$). **L, M** Serum levels of total cholesterol and triglycerides ($n = 5$). (Data are presented as the mean \pm SEM, t-test between two groups, one-way ANOVA with Tukey's test, or two-way ANOVA with Sidak's test between multiple groups. * $p < 0.05$, ** $p < 0.01$, *** $p < 0.001$, **** $p < 0.0001$, ns no significance).

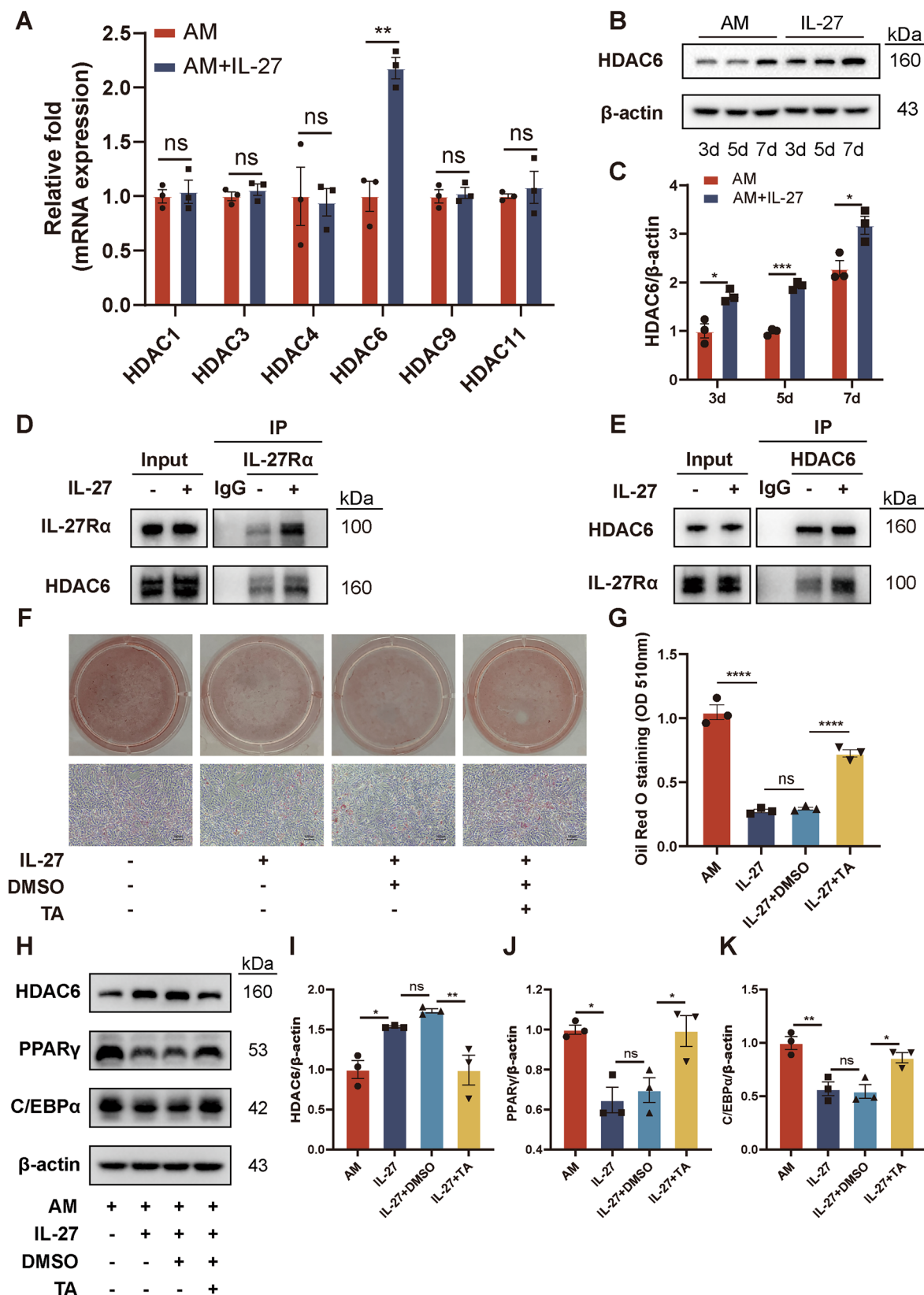


Fig. 4 | IL-27 inhibits adipogenic differentiation of ADSCs through HDAC6.

A Relative mRNA expression levels of the HDACs family ($n = 3$). **B, C** Western blot bands and IOD analysis of HDAC on days 3, 5, and 7 of adipogenic differentiation ($n = 3$). **D, E** Co-IP experiments reveal that IL-27 promotes the interaction between IL-27 α and HDAC6 in C3H10T1/2 cell lines. **F, G** Oil Red O staining and quantification on day 7 of adipogenic differentiation with IL-27 and the HDAC6-specific inhibitor Tubastatin A (TA). ($n = 3$, Scale bar = 100 μ m). **H–K** Western blot bands

and IOD analysis of HDAC6, PPAR γ , and C/EBP α on day 7 of adipogenic differentiation with IL-27 and TA ($n = 3$). (C3H10T1/2 cells were used exclusively in the Co-IP assay, while ADSCs were used for all other experiments. Data are presented as the mean \pm SEM, t-test between two groups, one-way ANOVA with Tukey's test between three or more groups. * $p < 0.05$, ** $p < 0.01$, *** $p < 0.001$, **** $p < 0.0001$, ns no significance).

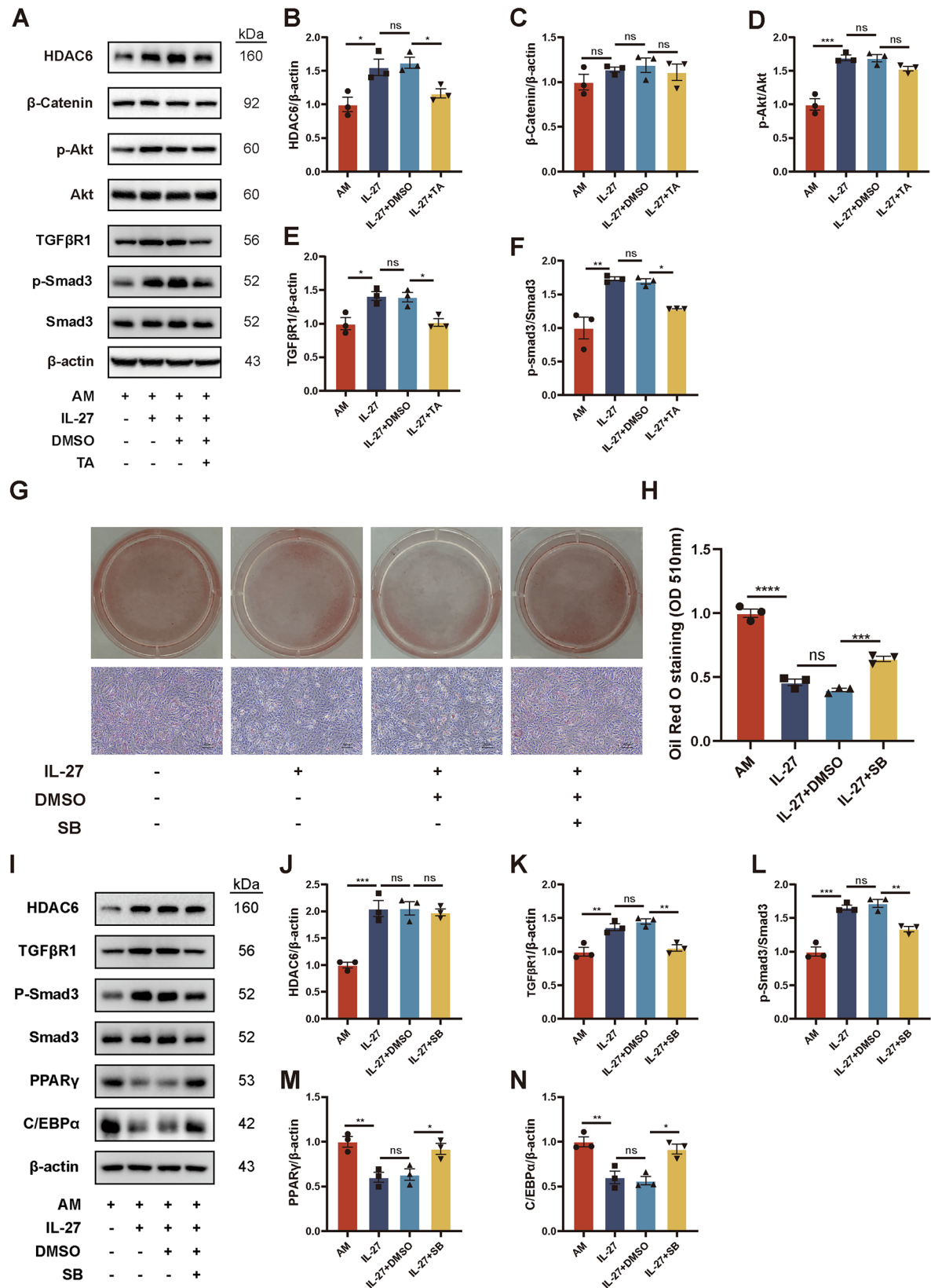


Fig. 5 | IL-27 inhibits adipogenic differentiation through the HDAC6-mediated activation of the TGFβ/Smad3 pathway in vitro. On day 7, IL-27 was reintroduced during the medium change, and samples were collected 6 hours later. **A–F** Western blot bands and IOD analysis of pathway effector proteins β-Catenin, p-Akt, and p-Smad3 during adipogenic differentiation (n = 3). **G, H** Oil Red O staining and quantification on day 7 of adipogenic differentiation with IL-27 and the TGFβ/

Smad3 pathway-specific inhibitor SB-431542 (SB). (n = 3, scale bar = 100 μm). **I–N** Western blot bands and IOD analysis of HDAC6, TGFβR1, p-Smad3, PPARγ, and C/EBPα on day 7 of adipogenic differentiation with IL-27 and SB (n = 3). (Data are presented as the mean ± SEM, t-test between two groups, one-way ANOVA with Tukey's test between three or more groups. *p < 0.05, **p < 0.01, ***p < 0.001, ****p < 0.0001, ns no significance).

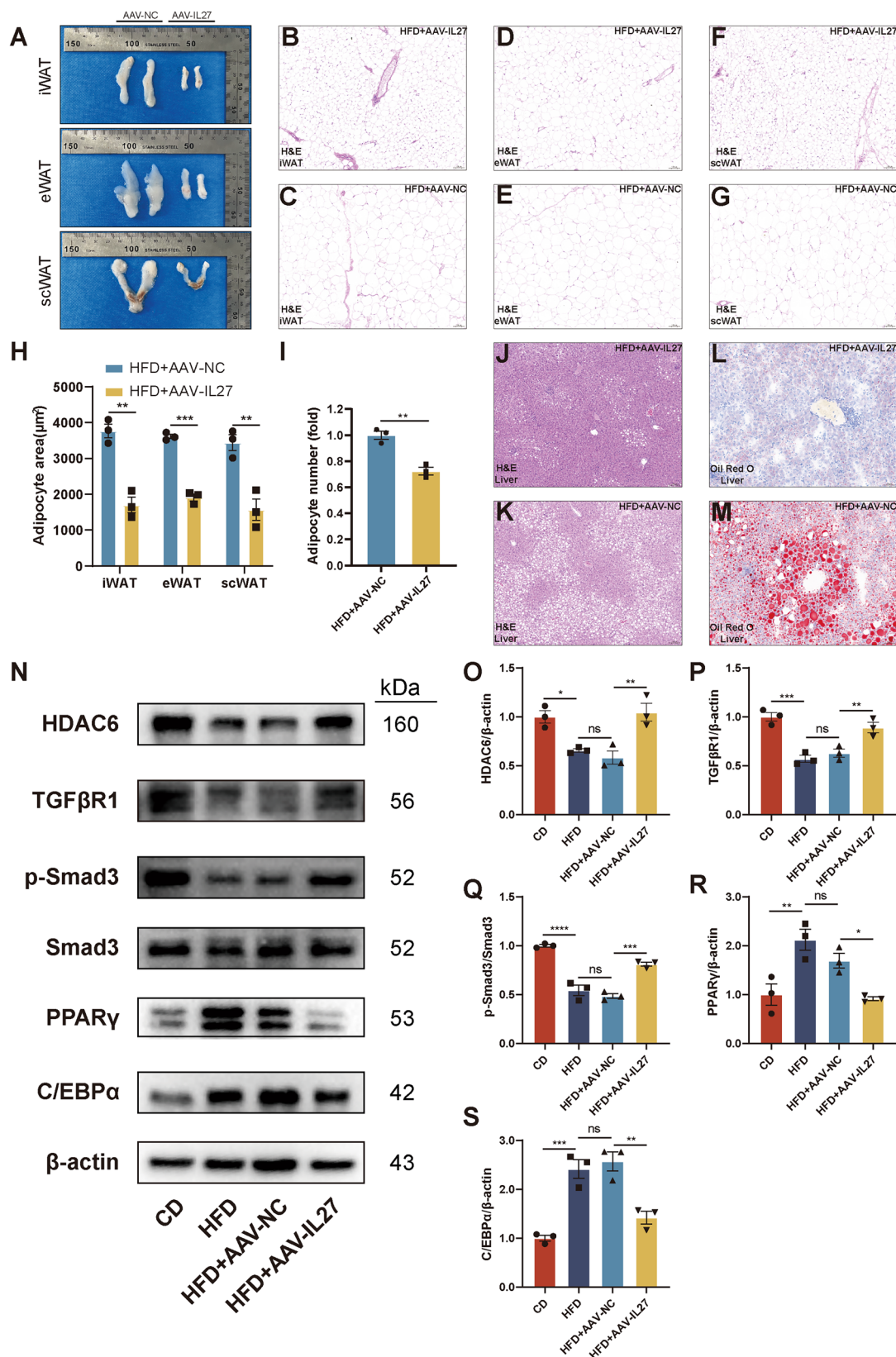


Fig. 6 | IL-27 inhibits adipogenesis through the HDAC6/TGFβ/Smad3 pathway in vivo. Male C57BL/6J mice were randomly assigned to the HFD + AAV-NC or HFD + AAV-IL27 groups. At the start of the experiment, adeno-associated virus overexpression or control vectors were administered via tail vein injection. HFD feeding continued for 12 weeks. **A** Representative photographs of inguinal, epididymal, and scapular white adipose tissues (iWAT, eWAT, and scWAT). **B–I** H&E staining and quantitative analysis of adipocyte area and number in iWAT, eWAT,

and scWAT. (n = 3, scale bar = 100 μm). **J–M** H&E (scale bar = 100 μm) and Oil Red O (scale bar = 50 μm) staining of the liver. **N–S** Western blot bands and IOD analysis of HDAC6, TGFβR1, p-Smad3, PPARγ, and C/EBPα in adipose tissues in vivo (n = 3). (Data are presented as the mean ± SEM, t-test between two groups, one-way ANOVA with Tukey's test between three or more groups. *p < 0.05, **p < 0.01, ***p < 0.001, ****p < 0.0001, ns no significance).

white adipose tissue expansion and improved metabolic homeostasis in HFD-fed mice. These findings suggest that IL-27 exerts an inhibitory effect on ADSC adipogenesis through HDAC6-mediated activation of the TGF β /Smad3 signaling pathway.

IL-27 exhibits infection-dependent dual inflammatory effects that depend on the environment. While immune cells are the main producers of IL-27, it is worth noting that non-immune cells, including adipocytes, can also synthesize IL-27³⁴. Obese individuals have much lower levels of circulating IL-27 than lean individuals do (about 200 pg/ml vs. 700 pg/ml, respectively)¹⁸. Consistently, we found reduced serum IL-27 levels in HFD-fed obese mice. Furthermore, *in vitro* experiments demonstrated that IL-27 signaling transcription levels were downregulated during adipogenesis process, aligning with previous study. The significance of IL-27 in obesity and metabolic illnesses has garnered increased attention. Studies indicate that IL-27 signaling deficiency exacerbates the incidence of streptozotocin-induced diabetes in mice, whereas exogenous recombinant IL-27 can restore hyperglycemia in the EBI3^{-/-} mouse model but not in the IL-27R α ^{-/-} mice³⁵. Our study found that targeted overexpression of IL-27 in adipose tissue effectively improved glucose and lipid metabolism disorders induced by HFD and significantly reduced adipose tissue content. Food intake is a crucial factor in obesity development³⁶. Zhang et al. indicated that administering exogenous IL-27 directly into the hypothalamus of mice resulted in a reduction in ghrelin and food consumption³⁷. However, we did not observe changes in food intake in HFD-fed mice, possibly due to our use of an adipose tissue-specific IL-27 overexpression viral vector, which avoids IL-27's effects on other tissues or organs.

IL-27 is considered a promising therapeutic target for obesity. Studies have found that IL-27 can enhance the production of UCP1 in brown adipose tissue, enhancing thermogenesis in adipocytes^{17,18}. However, its role in adipogenesis remains unclear. Adipogenesis is a complex process tightly regulated by a series of specific transcription factors, notably PPAR γ and C/EBP α ³⁸, which activate a cascade of adipogenic genes containing C/EBP and PPAR regulatory elements in their promoters³⁹. We found that IL-27 significantly inhibits the expression of PPAR γ and C/EBP α . HDACs, acting as transcriptional repressors, can inhibit the transcriptional activity of adipogenic transcription factors⁴⁰. HDACs can regulate the expression of interleukins and are reciprocally regulated by them^{27,41}. Studies have shown that increased HDAC6 activity can inhibit primary cilia elongation and adipocyte differentiation through regulation of α -tubulin acetylation⁴². Given the connection between interleukins and HDACs, we examined the expression levels of various HDAC family members. Our results indicate that IL-27 can upregulate HDAC6 expression and promote interaction between IL-27R α and HDAC6, suggesting that HDAC6 may serve as an adapter protein in IL-27 signal transduction.

The TGF β /Smad signaling pathway plays a crucial role in regulating adipogenesis^{28,43}. TGF β has been shown to inhibit adipocytes formation from mesenchymal stem cells by suppressing PPAR γ and C/EBP α transcription⁴⁴. Phosphorylation and nuclear accumulation of Smad3 are regulated by HDAC6⁴⁵. Our study found that HDAC6 activates the TGF β /Smad3 signaling pathway, possibly through modulation of TGF β R1. Additionally, we examined other important signaling pathways involved in adipocyte differentiation, such as Wnt/ β -catenin and PI3K/Akt^{19,29}. Specifically, IL-27 can upregulate p-Akt levels, which are not reversed by HDAC6-specific inhibitors and do not alter β -catenin levels. To further elucidate the role of the TGF β /Smad3 signaling pathway in ADSC adipogenic differentiation, we enhanced adipogenic differentiation by inhibiting this pathway with SB, demonstrating that activation of the TGF β /Smad3 signaling pathway inhibits adipogenic differentiation.

Further studies are needed to better understand the mechanisms of IL-27 in treating obesity. Due to ethical limitations, obtaining human-derived ADSCs is challenging, so we relied on analysis from the GEO database. Notably, other studies have found that macrophages also specifically express FABP4, which may lead to off-target effects of AAV-overexpressed IL-27⁴⁶. However, some studies have shown that FABP4-Cre is expressed only in adipose tissue, with no detection in the liver, heart, skeletal muscle, or

macrophages⁴⁷. Regardless, our experiments demonstrate that IL-27 can inhibit adipogenesis, and this conclusion is not influenced by other factors. Moreover, as IL-27 is a dual-function inflammatory factor⁴⁸, while we have shown that IL-27 inhibits adipogenesis, its regulation of adipose tissue inflammation or its effects on other tissues remain to be further explored.

Our study demonstrates that IL-27 can inhibit adipogenesis, suppress weight gain, and improve the balance of glucose and lipid metabolism through the activation of the HDAC6-mediated TGF β /Smad3 signaling pathway in HFD mice. Our findings suggest that IL-27 is a potential target for the treatment of obesity and related metabolic disorders. Nevertheless, additional investigation may be necessary to comprehensively comprehend its mechanisms and long-term effects.

Materials and methods

Analysis of Gene Expression Omnibus (GEO) database

We retrieved the GEO database with specific criteria: 1) Limited to Homo sapiens, 2) Availability of ADSCs adipogenic differentiation time series data, and 3) mRNA expression profiles. We selected datasets GSE125331, GSE198481, and GSE249195 for analysis^{19–21}. All three datasets pertain to adipogenic differentiation of human adipose-derived mesenchymal stem cells. Differential gene screening was performed using the GEO2R online tool (www.ncbi.nlm.nih.gov/geo/geo2r) under conditions of $p < 0.05$ and $|\log_2FC| \geq 2$. Volcano plots of differential genes were generated using R (Version 4.3.3), and common differential genes among the three datasets were identified using the “VennDiagram” R package (Version 1.7.3).

Isolation, culture, and adipogenic differentiation of ADSCs

Primary ADSCs were isolated from subcutaneous adipose tissue of 5-week-old male C57BL/6 J mice. The tissue was then cut into pieces approximately 0.5–1 mm³ in size and digested with 0.1% type II collagenase in a shaking water bath at 37°C until fully dissolved. The digestion was terminated and centrifuged to obtain the cell pellet. Next, Cell pellets were filtered using a 70 μ m cell strainer and then inoculated into culture flasks containing 10% fetal bovine serum (FBS) and 1% penicillin/streptomycin in Dulbecco's Modified Eagle's Medium Nutrient Mixture F-12 (DMEM/F12). The first medium change was performed after 48 hours, and subsequently, the medium was changed every 3 days. Cells were passaged at 80–90% density. Cells obtained from passages 3 to 5 were utilized for future investigations.

The C3H10T1/2 mesenchymal stem cell line was purchased from Procell (Wuhan, China) and cultured in a specialized culture medium (Procell, Wuhan, China) at a temperature of 37°C in an environment containing 5% CO₂.

For adipogenic differentiation, cells were grown to 100% confluence. Two days post-confluence, adipogenic differentiation was induced using high-glucose DMEM containing 10% FBS and an MDI cocktail (100 μ M indomethacin, 10 μ g/mL insulin, 0.5 mM 3-isobutyl-1-methylxanthine, and 1 μ M dexamethasone, all from Sigma)⁴⁹. The cells were cultured in induction medium for 3 days, followed by maintenance medium for 2 days, with alternating medium changes until lipid droplet were clearly formed. IL-27 treatment was refreshed with each medium change. On day 7, IL-27 was reintroduced during the medium change, and samples were collected 6 hours later for subsequent experiments.

Recombinant mouse IL-27 was purchased from Biolegend (San Diego, CA). The Dimethyl sulfoxide, the HDAC6-specific inhibitor TA, and the TGF β /Smad signaling pathway inhibitor SB were purchased from MCE (New Jersey, USA).

Cytotoxicity assay

The impact of IL-27 on the proliferation of ADSCs was evaluated using the Cell Counting Kit-8 (CCK-8) assay. ADSCs were cultured in 96-well dishes with a density of 3×10^3 cells per well. After 24 hours, once the cells adhered, different concentrations of IL-27 (0, 25, 50, 100, and 200 ng/mL) were added. At 24, 48, 72, and 96 hours, 10% CCK-8 reagent (Dojindo Molecular Technologies, Japan) was added to 96-well dishes, incubated for 2 hours at 37°C, and the absorbance was measured at 450 nm. The impact of IL-27 on

cell proliferation was further examined using the 5-ethynyl-2'-deoxyuridine (EdU) assay. BeyoClick™ EdU-488 (Beyotime, China) was used for the experiment, following the directions provided by the manufacturer.

Plasmid construction and transfection

Mus-IL-27Rα-3xHA and Mus-HDAC6-3xFlag overexpression plasmids were constructed by IGEBio (Guangzhou, China). C3H10T1/2 cells were cultured in 100 mm dishes to achieve 70%-80% confluency for transfection. The plasmid was diluted in Opti-MEM serum-free medium (Gibco, USA) and mixed thoroughly. Immediately, Polyethylenimine Linear MAX (PEI, Yeasen, China) was added to the diluted plasmid solution and mixed gently. The mixture was incubated at room temperature for 15 minutes to form the plasmid-PEI transfection complex. Old growth medium was replaced with fresh, pre-warmed serum-free medium and the transfection complex was introduced. After 6 hours, the medium was substituted with a complete growth medium, and the cells were cultured for subsequent experiments.

Flow cytometry

ADSCs surface markers were analyzed by flow cytometry at passage 3 (1×10^6 /mL) using antibodies: FITC-CD34 (Thermo Scientific, USA), FITC-CD29, FITC-90, PE-CD44, and PE-CD45 (All from BD Bioscience, USA). Flow cytometric analysis was performed by flow cytometer (BD LSR Fortessa, USA), and data was further analyzed using FlowJo v10.

Animals and treatments

C57BL/6J male mice (5-week-old, 16-20 g) were purchased from TopBio-tech Co., Ltd. (Shenzhen, China). Mice were housed in temperature- and humidity-controlled animal facilities (25 °C, 12-hour light/dark cycle) with free access to food and water. After one week of adaptive feeding on a standard chow diet (CD), 6-week-old mice were fed a 60% HFD (Research Diets, USA) for 12 weeks. An adeno-associated virus (AAV) vector for IL-27 overexpression targeting adipose tissue (AAV2/9-FABP4-IL27-3xFlag) and control vector (AAV2/9-FABP4-NC) were constructed by HanBio (Shanghai, China). At 6 weeks of age, each mouse received an intravenous injection of 1.9×10^{11} viral genomes via the tail vein⁵⁰. Subsequent experiments were conducted after 12 weeks of feeding on either a HFD or CD. Weekly measurements were taken for body weight and food intake. The QMR06-090H analyzer (Niumag, China) was applied to conduct body composition analysis.

Histology

Liver, inguinal, epididymal, and scapular white adipose tissues were collected and preserved in 4% paraformaldehyde solution. The samples were dehydrated through an ethanol gradient and fixed in paraffin. Sections were stained with hematoxylin for 5 minutes, dehydrated in graded alcohol, and then stained with eosin for 5 minutes. After alcohol dehydration, sections were sealed with neutral resin. For Oil Red O staining of the liver, fresh frozen liver tissue sections were prepared and brought to room temperature. Sections were stained with Oil Red O dye solution, differentiated with 60% isopropanol, counterstained with hematoxylin, and mounted using glycerin gelatin. The prepared slides were converted into digital format utilizing the Panoramic Scan 150 system for picture analysis.

For adipogenic differentiation of ADSCs, the medium was discarded, and the cells were gently washed twice with phosphate buffered saline (PBS). The cells were treated with 4% paraformaldehyde for half an hour. After discarding the paraformaldehyde, the cells were gently washed three times with PBS. Next, the Oil Red O dye solution (Formulated by combining the Oil Red O stock solution (Solarbio, China) and distilled water at a proportion of 3:2) was added to each well of a six-well dish. It took 20 minutes of staining the cells in the dark at room temperature. Subsequently, the cells were delicately washed with PBS. This study involves two methods for quantifying Oil Red O staining. The first method involves randomly capturing images of Oil Red O-stained samples under a light microscope, followed by measuring the stained area using ImageJ software. Second, the Oil Red O dye was extracted from the cells using 100% isopropanol (v/v).

The absorbance at 510 nm was measured to determine the amount of staining.

Adipocyte size and number

The prepared adipose tissue sections were digitized using the Panoramic Scan 150 system for detailed image analysis. The average diameter (d) of adipocytes was obtained using ImageJ software. The weight of a single adipocyte can be estimated based on its volume (approximated as a sphere, $\pi d^3/6$) and the density of adipose tissue (0.9 g/ml). The weight of adipose tissue in mice was determined using the QMR06-090H analyzer. The total number of adipocytes in the body was estimated by calculating the body fat weight and adipocyte volume distribution^{51,52}.

Glucose tolerance test (GTT) and insulin tolerance test (ITT)

To perform GTT, mice were given a 20% glucose solution (2 g/kg) intraperitoneally after a 12-hour fast. Blood glucose levels were measured at 30, 60, 90, and 120 mins. For ITT, a 4-hour fast was followed by an intraperitoneal dose of insulin (0.5 U/kg). Blood glucose levels were measured at 15, 30, 60, 90, and 120 mins. Fasting blood glucose levels before the procedures were taken as baseline. Blood glucose was measured from tail blood using a glucometer (Sinocare, China).

Blood biochemistry assay

Specimens were obtained and preserved at −80 °C. IL-27 levels were measured using a mouse IL-27 ELISA kit (Multisciences, China) following the guidelines provided by the manufacturer. Total cholesterol and total triglyceride levels were measured using the Total Cholesterol (TC) Colorimetric Assay Kit and Triglyceride (TG) Colorimetric Assay Kit (Elabscience, China), respectively, following the manufacturer's protocols.

RNA extraction and real-time quantitative PCR (qPCR) assays

RNA was extracted from cells using pre-cooled TRIzol reagent (Sigma, USA). After mixing with chloroform and performing high-speed centrifugation, isopropanol was used to obtain the RNA precipitate. Following the washing step with 75% ethanol, the RNA precipitate was dissolved in water that had been treated with diethyl pyrocarbonate. The manufacturer's protocol for the Evo M-MLV Reverse Transcription Premix Kit (Accurate Biology, China) was adopted. cDNA synthesis followed timing and temperature guidelines. The qPCR procedure was conducted according to the SYBR Green kit (Accurate Biology, China). Primer sequence details are shown in Supplementary Table 2. Using the Roche Diagnostic Light Cycler 480 System, Ct values were obtained by the established protocol procedures. The $2^{-\Delta\Delta Ct}$ method was used for relative quantitative analysis.

Western blot and co-immunoprecipitation (Co-IP)

Western blot was performed as previously described⁵³. The Co-IP assay was conducted using the Pierce Direct Magnetic IP/Co-IP Kit (Thermo Scientific, USA), following the directions provided by the manufacturer. The following antibodies were used: β-actin (Cell Signaling Technology, 4970), PPARγ (Cell Signaling Technology, 2435), CEBPα (Cell Signaling Technology, 8178), FABP4 (Cell Signaling Technology, 2120), HDAC6 (Cell Signaling Technology, 7612), p-Akt (Cell Signaling Technology, 4060), Akt (Cell Signaling Technology, 4691), β-catenin (Cell Signaling Technology, 8480), TGFβR1 (Proteintech, 30117-1-AP), p-Smad3 (Abcam, ab52903), Smad3 (Cell Signaling Technology, 9523), Anti-rabbit IgG HRP-linked Antibody (Cell Signaling Technology, 7074), Anti-mouse IgG HRP-linked Antibody (Cell Signaling Technology, 7076), DYKDDDDK (Proteintech, 66008-4-Ig), HA Tag (Proteintech, 66006-2-Ig).

Statistics and reproducibility

The data were processed and plotted using Prism 8.4.0 (GraphPad Software Inc., La Jolla, CA, USA). Each experiment was conducted with a minimum of three biological replicates. The Shapiro-Wilk method was used to test the normality of the data. Data are shown as mean ± standard error of the mean (mean ± SEM). Differences between two groups were analyzed using the

t-test. For multiple group comparisons, one-way ANOVA with Tukey's test or two-way ANOVA with Sidak's test was used. A p-value of <0.05 was considered statistically significant.

Data availability

Source data and unedited blot images can be obtained in Supplementary Data 1 and 2. Mus-HDAC6-3xFlag and Mus-IL-27R α -3xHA plasmid sequence deposited at Addgene (#235661, #235665). Data will be available from the corresponding author on reasonable request.

Received: 22 November 2024; Accepted: 11 March 2025;

Published online: 19 March 2025

References

- Kelly, T., Yang, W., Chen, C. S., Reynolds, K. & He, J. Global burden of obesity in 2005 and projections to 2030. *Int. J. Obes.* **32**, 1431–1437 (2008).
- Kahn, S. E., Hull, R. L. & Utzschneider, K. M. Mechanisms linking obesity to insulin resistance and type 2 diabetes. *Nature* **444**, 840–846 (2006).
- Van Gaal, L. F., Mertens, I. L. & De Block, C. E. Mechanisms linking obesity with cardiovascular disease. *Nature* **444**, 875–880 (2006).
- Tan, H. L. et al. Human amniotic mesenchymal stem cells-conditioned medium protects mice from high-fat diet-induced obesity. *Stem Cell. Res. Ther.* **12**, 364 (2021).
- Ghaben, A. L. & Scherer, P. E. Adipogenesis and metabolic health. *Nat. Rev. Mol. Cell Biol.* **20**, 242–258 (2019).
- Rodeheffer, M. S., Birsoy, K. & Friedman, J. M. Identification of white adipocyte progenitor cells in vivo. *Cell* **135**, 240–249 (2008).
- Cai, H. & Guo, H. Mesenchymal stem cells and their exocytotic vesicles. *Int. J. Mol. Sci.* **24**, 2085 (2023).
- Rosen, E. D. et al. C/EBP α induces adipogenesis through PPAR γ : a unified pathway. *Genes Dev.* **16**, 22–26 (2002).
- Abdalla, A. E., Li, Q., Xie, L. & Xie, J. Biology of IL-27 and its role in the host immunity against mycobacterium tuberculosis. *Int. J. Biol. Sci.* **11**, 168–175 (2015).
- Hunter, C. A. & Kastelein, R. Interleukin-27: balancing protective and pathological immunity. *Immunity* **37**, 960–969 (2012).
- Gong, H. et al. Dendritic cell-derived IL-27 p28 regulates T cell program in pathogenicity and alleviates acute graft-versus-host disease. *Signal Transduct. Target Ther.* **7**, 319 (2022).
- Silva, W. A. Jr. et al. The profile of gene expression of human marrow mesenchymal stem cells. *Stem Cells* **21**, 661–669 (2003).
- He, H. et al. Aging-induced IL27R α signaling impairs hematopoietic stem cells. *Blood* **136**, 183–198 (2020).
- Bobhate, A., Viswanathan, V. & Aravindhan, V. Anti-inflammatory cytokines IL-27, IL-10, IL-1R α and TGF- β in subjects with increasing grades of glucose intolerance (DM-LTB-2). *Cytokine* **137**, 155333 (2021).
- Wen, Y. et al. Serum IL-27 levels increase in subjects with hypothyroidism and are negatively correlated with the occurrence of nonalcoholic fatty liver disease. *Front. Endocrinol.* **14**, 1173826 (2023).
- Vargas-Alarcon, G. et al. Interleukin 27 polymorphisms, their association with insulin resistance and their contribution to subclinical atherosclerosis. The GEA Mexican study. *Cytokine* **114**, 32–37 (2019).
- Yang, Y., Liu, H. & Liu, D. Preventing high-fat diet-induced obesity and related metabolic disorders by hydrodynamic transfer of IL-27 gene. *Int. J. Obes.* **47**, 413–421 (2023).
- Wang, Q. et al. IL-27 signalling promotes adipocyte thermogenesis and energy expenditure. *Nature* **600**, 314–318 (2021).
- Yang Loureiro, Z. et al. Wnt signaling preserves progenitor cell multipotency during adipose tissue development. *Nat. Metab.* **5**, 1014–1028 (2023).
- Singh, A. M. et al. Human beige adipocytes for drug discovery and cell therapy in metabolic diseases. *Nat. Commun.* **11**, 2758 (2020).
- Kar, A. et al. Age-dependent genes in adipose stem and precursor cells affect regulation of fat cell differentiation and link aging to obesity via cellular and genetic interactions. *Genome Med.* **16**, 19 (2024).
- Shantaram, D. et al. Obesity-associated microbiomes instigate visceral adipose tissue inflammation by recruitment of distinct neutrophils. *Nat. Commun.* **15**, 5434 (2024).
- Almuraikhy, S. et al. Interleukin-6 induces impairment in human subcutaneous adipogenesis in obesity-associated insulin resistance. *Diabetologia* **59**, 2406–2416 (2016).
- Wan, X. et al. Shift work promotes adipogenesis via cortisol-dependent downregulation of EGR3-HDAC6 pathway. *Cell Death Discov.* **10**, 129 (2024).
- Ahmadi, S. et al. Impact of housing temperature on adipose tissue HDAC9 expression and adipogenic differentiation in high fat-fed mice. *Obesity* **32**, 107–119 (2024).
- Ferrari, A. et al. Inhibition of class I HDACs imprints adipogenesis toward oxidative and brown-like phenotype. *Biochim. Biophys. Acta Mol. Cell Biol. Lipids* **1865**, 158594 (2020).
- Shi, Y. et al. Requirement of histone deacetylase 6 for interleukin-6 induced epithelial-mesenchymal transition, proliferation, and migration of peritoneal mesothelial cells. *Front. Pharmacol.* **12**, 722638 (2021).
- Li, S. N. & Wu, J. F. TGF- β /SMAD signaling regulation of mesenchymal stem cells in adipocyte commitment. *Stem Cell. Res. Ther.* **11**, 41 (2020).
- Li, T. et al. Pomegranate flower extract bidirectionally regulates the proliferation, differentiation and apoptosis of 3T3-L1 cells through regulation of PPAR γ expression mediated by PI3K-AKT signaling pathway. *Biomed. Pharmacother.* **131**, 110769 (2020).
- Miura, A. et al. Conditional blastocyst complementation of a defective Foxa2 lineage efficiently promotes the generation of the whole lung. *Elife* **12**, e86105 (2023).
- Siniscalco, E. R. & Craft, J. IL-27 gives a good gut feeling about immune regulation. *Nat. Immunol.* **24**, 1972–1973 (2023).
- Xu, W. D., Wang, D. C., Zhao, M. & Huang, A. F. An updated advancement of bifunctional IL-27 in inflammatory autoimmune diseases. *Front. Immunol.* **15**, 1366377 (2024).
- Fuentes, E., Fuentes, F., Vilahur, G., Badimon, L. & Palomo, I. Mechanisms of chronic state of inflammation as mediators that link obese adipose tissue and metabolic syndrome. *Mediat. Inflamm.* **2013**, 136584 (2013).
- Shahi, A. et al. IL-27 and autoimmune rheumatologic diseases: the good, the bad, and the ugly. *Int. Immunopharmacol.* **84**, 106538 (2020).
- Fujimoto, H. et al. IL-27 inhibits hyperglycemia and pancreatic islet inflammation induced by streptozotocin in mice. *Am. J. Pathol.* **179**, 2327–2336 (2011).
- Bray, G. A. Obesity: a 100 year perspective. *Int. J. Obes.* **49**, 159–167 (2025).
- Zhang, H. et al. Interleukin-27 decreases ghrelin production through signal transducer and activator of transcription 3-mechanistic target of rapamycin signaling. *Acta Pharm. Sin. B.* **10**, 837–849 (2020).
- Wen, X. et al. Signaling pathways in obesity: mechanisms and therapeutic interventions. *Signal Transduct. Target Ther.* **7**, 298 (2022).
- MacDougald, O. A. & Lane, M. D. Transcriptional regulation of gene expression during adipocyte differentiation. *Annu. Rev. Biochem.* **64**, 345–373 (1995).
- Huang, Y. et al. Long Non-coding RNA H19 inhibits adipocyte differentiation of bone marrow mesenchymal stem cells through epigenetic modulation of histone deacetylases. *Sci. Rep.* **6**, 28897 (2016).
- Liao, W. T. et al. Histone deacetylase inhibitors attenuated interleukin-1 β -induced chondrogenesis inhibition in synovium-derived

- mesenchymal stem cells of the temporomandibular joint. *Bone Jt. Res.* **11**, 40–48 (2022).
42. Forcioli-Conti, N., Esteve, D., Bouloumie, A., Dani, C. & Peraldi, P. The size of the primary cilium and acetylated tubulin are modulated during adipocyte differentiation: analysis of HDAC6 functions in these processes. *Biochimie* **124**, 112–123 (2016).
 43. Shin, H. A., Park, M., Banga, J. P. & Lew, H. TGF β -treated placenta-derived mesenchymal stem cells selectively promote anti-adipogenesis in thyroid-associated ophthalmopathy. *Int. J. Mol. Sci.* **23**, 5603 (2022).
 44. Ahdjoudj, S. et al. Transforming growth factor-beta inhibits CCAAT/enhancer-binding protein expression and PPARgamma activity in unloaded bone marrow stromal cells. *Exp. Cell Res.* **303**, 138–147 (2005).
 45. Choi, S. Y. et al. Tubastatin A suppresses renal fibrosis via regulation of epigenetic histone modification and Smad3-dependent fibrotic genes. *Vasc. Pharmacol.* **72**, 130–140 (2015).
 46. Furuhashi, M. et al. Treatment of diabetes and atherosclerosis by inhibiting fatty-acid-binding protein aP2. *Nature* **447**, 959–965 (2007).
 47. He, W. et al. Adipose-specific peroxisome proliferator-activated receptor gamma knockout causes insulin resistance in fat and liver but not in muscle. *Proc. Natl. Acad. Sci. USA* **100**, 15712–15717 (2003).
 48. Aparicio-Siegmund, S. & Garbers, C. The biology of interleukin-27 reveals unique pro- and anti-inflammatory functions in immunity. *Cytokine Growth Factor Rev.* **26**, 579–586 (2015).
 49. Zhang, Z. et al. Obesity caused by an OVOL2 mutation reveals dual roles of OVOL2 in promoting thermogenesis and limiting white adipogenesis. *Cell Metab.* **34**, 1860–1874.e1864 (2022).
 50. Jimenez, V. et al. In vivo adeno-associated viral vector-mediated genetic engineering of white and brown adipose tissue in adult mice. *Diabetes* **62**, 4012–4022 (2013).
 51. Salans, L. B., Cushman, S. W. & Weismann, R. E. Studies of human adipose tissue. Adipose cell size and number in nonobese and obese patients. *J. Clin. Invest.* **52**, 929–941 (1973).
 52. Svensson, H. et al. Body fat mass and the proportion of very large adipocytes in pregnant women are associated with gestational insulin resistance. *Int. J. Obes.* **40**, 646–653 (2016).
 53. Hong, Y. et al. Elabela inhibits TRAF1/NF-kappaB induced oxidative DNA damage to promote diabetic foot ulcer wound healing. *iScience* **26**, 107601 (2023).

Acknowledgements

This work was supported by grants provided by the National Natural Science Foundation of China (No. 81070125, 81270213, 81670306); the Science and Technology Foundation in Guangdong Province (2014A020211002); the National Natural Science Foundation of Guangdong Province (No. 2017A030313503); the Science and Technology Foundation in Guangzhou City (No. 201806020084); Guangdong Basic and Applied Basic Research Foundation (2023A1515220199); the Fundamental Research Funds for the Central Universities (No. 13ykzd16, 17ykjc18); the Futian District Health and Public Welfare Research Project of Shenzhen City (No. FTWS2019001, FTWS2021016, FTWS2022018, FTWS2023064), the Shenzhen Science and Technology Program (No. JCYJ20190808101405466,

JCYJ20210324115003008, JCYJ20220530144404009, KCXFZ20230731094100002).

Author contributions

Conceived and designed the study: Yinsheng Zhong, Yajie Guo and Tong Wang. Performed the experiment: Yinsheng Zhong and Shujun Yang. Performed statistical analyses and visualization: Shuangmei Li and Xuxiang Chen. Collected and organized data: Sijun Yuan, Huibao Long and Haidong Wu. Wrote the first version of draft: Yinsheng Zhong and Yajie Guo. All authors read and approved the final manuscript.

Competing interests

The authors declare no competing interests.

Ethical approval

All animal procedures were approved by the Animal Ethics Committee of the Eighth Affiliated Hospital of Sun Yat-sen University (No. 2022-068-01).

Additional information

Supplementary information The online version contains supplementary material available at <https://doi.org/10.1038/s42003-025-07918-y>.

Correspondence and requests for materials should be addressed to Yajie Guo or Tong Wang.

Peer review information *Communications Biology* thanks the anonymous reviewers for their contribution to the peer review of this work. Primary Handling Editor: Mengtan Xing.

Reprints and permissions information is available at <http://www.nature.com/reprints>

Publisher's note Springer Nature remains neutral with regard to jurisdictional claims in published maps and institutional affiliations.

Open Access This article is licensed under a Creative Commons Attribution-NonCommercial-NoDerivatives 4.0 International License, which permits any non-commercial use, sharing, distribution and reproduction in any medium or format, as long as you give appropriate credit to the original author(s) and the source, provide a link to the Creative Commons licence, and indicate if you modified the licensed material. You do not have permission under this licence to share adapted material derived from this article or parts of it. The images or other third party material in this article are included in the article's Creative Commons licence, unless indicated otherwise in a credit line to the material. If material is not included in the article's Creative Commons licence and your intended use is not permitted by statutory regulation or exceeds the permitted use, you will need to obtain permission directly from the copyright holder. To view a copy of this licence, visit <http://creativecommons.org/licenses/by-nc-nd/4.0/>.

© The Author(s) 2025